

Comments to the Author:

While the major technical issues have been tackled, there are many English errors or non-standard usages. I just read the title and abstract. A dozen of such problems were noted, as listed below. The paper must be thoroughly edited to drastically improve its English, or it'd be rejected.

Response:

We would like to heartily thank you for your serious review on our work and the valuable comments. We revised the manuscript in accordance with your kind advices and detailed suggestions, and carefully proof-read the manuscript to minimize typographical, grammatical, and bibliographical errors and improve the English in the manuscript. Here below is our description on revision according to your comments. We sincerely hope the correction will meet with approval.

Comment 1: The title is misleading, change to “Evaluating the performance of two surface layer schemes for the momentum and heat exchange processes during severe haze pollution in Jing-Jin-Ji in east China”

Response:

Thanks for pointing this out, and we have changed the title according to the editor's advice.

Comment 2: “Pollutants prediction by atmosphere chemical model exists obvious deficiencies,” change to “There have existed some deficiencies in the prediction of pollutants by atmosphere chemical models”

Response:

We have revised the sentence in Lines 21-22, and other similar sentences in Lines 51, 56 have also been revised.

Comment 3: “The differences of two...” should be “The differences between two”

Response:

We changed “of” to “between” in this sentence in Line 24. We also revised similar mistakes in Line 33, Line 170, Line 311, Line 371 and Line 384.

Comment 4: “was mainly evaluated 22 based on”. To “was evaluated mainly based on ...”

Response:

Thank you for your advice. We put “mainly” before “evaluated” to illustrate that we evaluated the performances of the two schemes not only for the pollution process but also for the other times. “mainly” is for “a heavy haze episode”, not for “the observed momentum and sensible heat fluxes”. So we think it would be more appropriate to put “mainly” before “evaluated”. We revised this sentence to make the meaning more clear, and the revision is in Lines 24~26.

Comment 5: “play a major role in the flux calculation” to “play major roles in the flux calculation”

Response:

We changed “play a major role” to “play the major roles” in Line 27. We also corrected other places about singular and plural forms, such as in Line 89, Line 91, Line 272, and Line 335.

Comment 6: “Besides the roughness lengths” to “Besides the roughness length”

Response:

Thanks for pointing this out and we changed “roughness lengths” to “roughness length” as it is a concept here.

Comment 7: “the algorithms of universal functions for” either to “the algorithms for” or “the universal functions for” not both algorithms and functions.

Response:

Thanks for the editor's kind advice. We have deleted "of universal functions" in Line 30.

Comment 8: "magnitude of z_{0_m} and z_{0_h} has" to "the magnitudes of z_{0_m} and z_{0_h} have"

Response:

We have revised this mistake in Line 31.

Comment 9: Change all "compared with" to "comparing with"

Response:

We have changed all "compared with" to "comparing with" in the revised manuscript.

Comment 10: "Li scheme better characterized" to "Li scheme is better in characterizing"

Response:

We have revised this mistake in Line 34, and other similar parts were also revised.

Comment 11: "in the describing of" to either "in the description of" or "in describing .."

Response:

Thanks for pointing this mistake out, we have revised all similar problems in whole manuscript.

Evaluating the performance of two surface layer schemes for the momentum and heat exchange processes during severe haze pollution in Jing-Jin-Ji in easterneast China~~Evaluating study of the momentum and heat exchange process of two surface layer schemes during severe haze pollution in Jing-Jin-Ji in east China~~

Yue Peng^{1,2}, Hong Wang^{1,2}, Yubin Li³, Changwei Liu³, Tianliang Zhao², Xiaoye Zhang¹, Zhiqiu Gao^{3,4}, Tong Jiang⁵, Huizheng Che¹, Meng Zhang⁶

¹ State Key Laboratory of Severe Weather/Institute of Atmospheric Composition, Chinese Academy of Meteorological Sciences (CMAS), Beijing 100081, China

² Collaborative Innovation Center on Forecast and Evaluation of Meteorological Disasters/Key Laboratory for Aerosol-Cloud-Precipitation of China Meteorological Administration, Nanjing University of Information Science and Technology, Nanjing 210044, China

³ Key Laboratory of Meteorological Disaster of Ministry of Education/Collaborative Innovation Center on Forecast and Evaluation of Meteorological Disasters, School of [Atmospheric Physics Remote Sensing and Geomatics Engineering](#), Nanjing University of Information Science and Technology, Nanjing 210044, China

⁴ State Key Laboratory of Atmospheric Boundary Layer Physics and Atmospheric Chemistry, Institute of Atmospheric Physics, Chinese Academy of Sciences, Beijing 100029, China

⁵ National Climate Center, China Meteorological Administration, Beijing 100081, China

⁶ Beijing Meteorological Service, Beijing 100089, China

Correspondence to: Hong Wang (wangh@cma.gov.cn)

Abstract. The turbulent flux parameterization schemes in the surface layer are crucial for air pollution modeling. ~~There have existed some deficiencies in the Pollutants~~ prediction of air pollutants by atmosphere chemical models ~~exists obvious deficiencies~~, which ~~may be~~ closely related to the uncertainties of the momentum and sensible heat fluxes calculated in the surface layer. The differences ~~of~~ between two surface layer schemes (~~the~~ Li and MM5 schemes) were discussed, and the performances of the two schemes ~~focusing on a heavy haze episode was~~ ~~ere~~ mainly evaluated based on the observed momentum and sensible heat fluxes ~~during a heavy haze episode~~ in Jing-Jin-Ji in eastern China. The results showed that the aerodynamic roughness length z_{0m} and the thermal roughness length z_{0h} played ~~the~~ major roles in the flux calculation. ~~Compared~~ ~~Comparing~~ with the Li scheme, ignoring the difference between z_{0m} and z_{0h} ~~the two~~ in the MM5 scheme induced a great error in the calculation of sensible heat flux (e.g., the error was 54 % at Gucheng station). Besides the roughness lengths, the algorithms ~~of universal functions~~ for surface turbulent fluxes as well as the roughness sublayer also resulted in certain errors in the MM5 scheme. In addition, magnitudes of z_{0m} and z_{0h} ~~has~~ ~~ve~~ significant influence on the two schemes. The large z_{0m} and z_{0m}/z_{0h} in megacity with rough surface (e.g., Beijing) resulted in much larger differences of momentum and sensible heat fluxes ~~by~~ between Li and MM5, ~~compared~~ ~~comparing~~ with the small z_{0m} and z_{0m}/z_{0h} in suburban area with smooth surface (e.g., Gucheng). The Li scheme ~~could~~ ~~is~~ better in characterizing the evolution of atmospheric stratification than the

35 MM5 scheme in general, especially for the transition stage from unstable to stable atmospheric stratification corresponding to
36 the PM_{2.5} accumulation. The bias~~es~~ of momentum and sensible heat fluxes from Li were lower about 38 % and 43 %
37 respectively than those from MM5 during this stage. This study indicates the superiority of the Li scheme in ~~the describing of~~
38 the regional atmospheric stratification, ~~and also suggests the with~~ improving possibility of severe haze prediction in Jing-Jin-
39 Ji in east~~ern~~ China by coupling it into ~~the~~ atmosphere chemical models ~~online~~.

40 **Key words:** surface layer; turbulent flux parameterization; roughness length; numerical modeling; air pollution

41 1 Introduction

42 Adequate air quality modeling relies on accurate simulation of meteorological conditions, especially in the planetary
43 boundary layer (PBL) (Hu et al., 2010; Cheng et al., 2012; Xie et al., 2012). The PBL is tightly coupled ~~to~~with the earth's
44 surface by turbulent exchange processes. As the bottom layer of PBL, the surface layer (SL) reflects the surface state by
45 calculating momentum, heat, water vapor and other fluxes, and influences the atmospheric structure by turbulent transport
46 process. Many studies have illustrated the important roles of meteorological factors in the SL ~~during in the formation of~~ air
47 pollution ~~formation~~. ~~It has been~~They demonstrated that weak wind speed, high relative humidity (RH) and strong temperature
48 inversion are favorable for the haze concentrating (Zhang et al., 2014; Yang et al., 2015; Liu et al., 2017; Zhong et al., 2017).
49 The strong stable stratification and weak turbulent are mainly responsible for many haze events. The relationship between flux
50 and atmospheric profile in the atmospheric surface layer is a critical factor for air pollution diffusion, especially under stable
51 stratification conditions (Li et al., 2017). However, ~~there are the study of stable boundary layer~~ still ~~has~~ some uncertainties ~~in~~
52 ~~the study of stable boundary layer~~ due to the poor description of surface turbulent motion. The simulating study on a severe
53 haze in east~~ern~~ China by the Weather Research and Forecasting/Chemistry (WRF-Chem) model concluded that ~~there is lower~~
54 ~~ability of~~ current PBL schemes ~~hads a weak ability to~~ distinguish ~~ing the diffusion~~ between haze days under stable conditions
55 and clean days under unstable conditions (Li et al., 2016a). Another study (Vautard et al. 2012) ~~enof~~ mesoscale meteorological
56 models also pointed out ~~there was~~ a systematic overestimation of near-surface wind speed in ~~thea~~ stable boundary layer ~~which~~
57 ~~and its possible should~~ contribute ~~cion~~ to the underestimation of ~~the PM_{2.5} pollution surface concentrations of primary pollutions~~.
58 In addition, atmospheric conditions in both the PBL and upper layers are highly dependent on ~~the~~ turbulent fluxes which are
59 computed in the SL (Ban et al., 2010). Flux parameterization in the SL plays an important role in studies of the hydrological
60 cycle and weather prediction (Yang et al., 2001; Li, 2014). An adequate SL scheme is crucial to provide an accurate
61 atmospheric evolution by numerical models (Jiménez et al., 2012) and hence it may introduce significant impacts on air
62 pollution simulation.

63 The bulk aerodynamic formulation based on Monin-Obukhov similarity theory (hereinafter MOST, Monin and Obukhov,
64 1954) is usually employed to calculate surface fluxes in numerical models. Turbulent fluxes are parameterized by wind,

65 temperature, humidity in the lowest layer in the model and temperature and humidity at the surface. Many international scholars
66 verified the MOST using field experiments and then proposed the universal functions, the commonly used of which is
67 Businger-Dyer (BD) equation (Businger, 1966; Dyer, 1967). With the development of observation technology, the coefficients
68 in the BD equation have been further modified (Paulson, 1970; Webb, 1970; Businger et al., 1971; Dyer, 1974; Högström,
69 1996). In addition to the BD equation, some other schemes have been put forward and they performed better especially for
70 strongly stable stratification (Holtslag and De Bruin, 1988; Beljaars and Holtslag, 1991; Cheng and Brutsaert, 2005). The
71 schemes can be divided into two types according to the computing characteristics. One type is called as iterative algorithm
72 (Paulson, 1970; Businger et al., 1971; Dyer, 1974; Högström, 1996; Beljaars and Holtslag, 1991), and it keeps the MOST
73 completely with less approximation so that the results can be more precise. However, it needs to take much more steps to
74 converge and hence the CPU time is consuming which reduces the computational efficiency of modeling (Louis, 1979; Li et
75 al., 2014); The other one is called as non-iterative algorithm (Louis et al., 1982; Launiainen, 1995; Wang et al., 2002; Wouters
76 et al., 2012). There is no requirement for loop iteration in the calculation due to the approximate treatment. This algorithm is
77 much simpler and less CPU time-consuming, but the results are based on the loss of the calculation accuracy.

78 A new non-iterative scheme proposed by Li et al. (2014; 2015, Li hereinafter) speeds up effectively under a higher
79 accuracy ~~compared-comparing~~ with some classic iterative computation. It is remarkable that this new scheme just has been
80 theoretically evaluated and it has never been applied in any models. Haze pollution occurs frequently in recent years in eastern
81 China. The concentration of PM_{2.5} may reach up to 1000 μg m⁻³ in the Beijing-Tianjin-Hebei (Jing-Jin-Ji) region in winter
82 (Wang et al., 2014) while it ~~is-was~~ generally underestimated by current air quality models (Zhang et al., 2015; Li et al., 2016a;
83 Liu et al., 2017). The Li and another classic SL scheme (Zhang and Anthes, 1982, MM5 hereinafter) ~~are-were~~ compared in
84 details in this study. The observed momentum and sensible heat flux data covering one complete haze process at Gucheng
85 station were used to evaluate the two schemes focusing on the transition stage from unstable to stable atmospheric stratification
86 corresponding to the PM_{2.5} accumulation. The evaluation is in the view of both local and regional scales. This ~~offline~~-study
87 may provide the prerequisite for ~~the-online~~ coupling the Li scheme into atmosphere chemical models in the future.

88 2 Theory

89 The definitions of momentum and sensible heat flux as well as the detailed algorithms of the Li and MM5 schemes are
90 introduced in this section.

91 2.1 Introduction of the momentum and sensible heat flux

92 The turbulent fluxes from ground surface are defined as follows:

$$93 \tau = \rho u_*^2, \quad (1a)$$

$$94 H = -\rho c_p u_* \theta_*, \quad (1b)$$

95 where τ is the momentum flux, H is the sensible heat flux, ρ is the air density, c_p is the specific heat capacity at constant
 96 pressure. u_* and θ_* are the friction velocity and the temperature scale, respectively, and they represent the intensity of the
 97 vertical turbulent flux transport and are approximately independent on height in the SL.

98 Both the Li and MM5 schemes are ~~calculated with~~based on bulk flux parameterization. As an important dimensionless
 99 parameter related to the stability, the bulk Richardson number Ri_B is defined as

$$100 \quad Ri_B = \frac{gz(\theta - \theta_g)}{\theta u^2}, \quad (2)$$

101 where g is the acceleration of gravity, z is the reference height which is the lowest level in ~~the models~~, θ is the mean potential
 102 temperature at height z , θ_g is the surface radiometric potential temperature, u is the mean wind speed at height z . Thus, Ri_B
 103 can be computed through meteorological variables from at least two levels.

104 2.2 The Li scheme

105 This new scheme employs non-iterative algorithm to compute the surface fluxes. Its basic idea is to parameterize the
 106 stability parameter ζ directly with Ri_B and roughness lengths (z_{0m} and z_{0h}). Specifically, bulk transfer coefficients of the
 107 momentum and sensible heat fluxes (C_M and C_H) are expressed as

$$108 \quad C_M = \frac{u_*^2}{u^2} = \frac{\tau}{\rho u^2}, \quad (3a)$$

$$109 \quad C_H = \frac{u_* \theta_*}{u(\theta - \theta_g)} = -\frac{H}{\rho c_p u(\theta - \theta_g)}. \quad (3b)$$

110 Based on MOST and considering the roughness sublayer (RSL) effect at the same time, the relationships between the
 111 bulk transfer coefficients and the profile functions corresponding to wind and potential temperature are usually expressed as

$$112 \quad C_M = \frac{k^2}{\left[\ln \frac{z}{z_{0m}} - \psi_M \left(\frac{z}{L} \right) + \psi_M \left(\frac{z_{0m}}{L} \right) + \psi_M^* \left(\frac{z}{L}, \frac{z}{z_*} \right) \right]^2}, \quad (4a)$$

$$113 \quad C_H = \frac{k^2}{R \left[\ln \frac{z}{z_{0m}} - \psi_M \left(\frac{z}{L} \right) + \psi_M \left(\frac{z_{0m}}{L} \right) + \psi_M^* \left(\frac{z}{L}, \frac{z}{z_*} \right) \right] \left[\ln \frac{z}{z_{0h}} - \psi_H \left(\frac{z}{L} \right) + \psi_H \left(\frac{z_{0h}}{L} \right) + \psi_H^* \left(\frac{z}{L}, \frac{z}{z_*} \right) \right]}, \quad (4b)$$

114 where k is the von Kármán constant which is 0.4 in both two schemes, R is the Prandtl number which is 1.0 in the two
 115 schemes, z_{0m} and z_{0h} are the aerodynamic roughness length and the thermal roughness length, respectively. ψ_M and ψ_H
 116 are the integrated stability functions for momentum and sensible heat, respectively, which are also called universal functions.

117 L is the Obukhov length ($\zeta = \frac{z}{L}$), ψ_M^* and ψ_H^* are the correction functions accounting for RSL effect, z_* is the RSL height.

118 It is clear to see that the calculation of the momentum and sensible heat fluxes requires C_M and C_H (or u_* and θ_*), and
 119 there are 3 key points to get them:

- 120 1. z_{0m} and z_{0h} . z_{0m} and z_{0h} are two key parameters in the bulk transfer equations. Their definitions and influences
 121 will be discussed in Sect. 4.1. Note that both z_{0m} and z_{0h} are taken into account by the Li scheme. In other words, the
 122 Li scheme distinguishes ~~these~~ two principal surface parameters effectively as they generate from different mechanisms.
- 123 2. ζ . The determination of ζ is the most crucial problem ~~for~~in the Li scheme. In fact, this new scheme consists of two

parts. The first part ~~was~~ proposed for atmospheric stable stratification condition ζ (Li et al., 2014), and the second part then extended the scheme to unstable condition ζ (Li et al., 2015). For stable condition ζ , the calculation procedure for a given group of Ri_B , z_{om} and z_{oh} is the following: (1) find the region according to z_{om} and z_{oh} ; (2) find the section according to the region and Ri_B with Eq. (5) and given coefficients; (3) calculate ζ using Eq. (6) and given coefficients.

$$Ri_{BCP} = \sum C_{mn} (\log L_{OM})^m (L_{OH} - L_{OM})^n, \quad (5)$$

$$\zeta = Ri_B \sum C_{ijk} Ri_B^i L_{OM}^j (L_{OH} - L_{OM})^k, \quad (6)$$

where C_{mn} and C_{ijk} are the coefficients listed in Tables in Li et al. (2014). $L_{OM} = \ln \frac{z}{z_{om}}$, $L_{OH} = \ln \frac{z}{z_{oh}}$. $m, n = 0, 1, 2$, and $m + n \leq 3$; $i, j, k = 0, 1, 2, 3$, and $i + j + k \leq 4$. Similarly, for unstable condition ζ , eight regions are divided according to the method from Li et al. (2015). For each of the regions, ζ is carried out by following:

$$\zeta = Ri_B \frac{L_{OM}^2}{L_{OH}} \sum C_{ijk} \left(\frac{-Ri_B}{1-Ri_B} \right)^i L_{OM}^{-j} L_{OH}^{-k}, \quad (7)$$

where C_{ijk} is listed in Li et al. (2016b), and $i = 0, 1$; $j, k = 0, 1, 2, 3$; $i + j + k \leq 4$.

3. Universal function. It is also a key factor in flux calculation. The form of universal function here is adopted from Cheng and Brutsaert (2005) under the stable condition ζ (Eqs. (8a), (8b)) and it is adopted from Paulson (1970) under the unstable condition ζ (Eqs. (9a), (9b)):

$$\psi_M(\zeta) = -a \ln \left[\zeta + (1 + \zeta^b)^{\frac{1}{b}} \right], \quad \zeta > 0 \text{ (stable)}, \quad (8a)$$

$$\psi_H(\zeta) = -c \ln \left[\zeta + (1 + \zeta^d)^{\frac{1}{d}} \right], \quad \zeta > 0 \text{ (stable)}, \quad (8b)$$

$$\psi_M(\zeta) = 2 \ln \frac{1+x}{2} + \ln \frac{1+x^2}{2} - 2 \arctan(x) + \frac{\pi}{2}, \quad \zeta < 0 \text{ (unstable)}, \quad (9a)$$

$$\psi_H(\zeta) = 2 \ln \frac{1+y}{2}, \quad \zeta < 0 \text{ (unstable)}, \quad (9b)$$

where $a = 6.1$, $b = 2.5$, $c = 5.3$, $d = 1.1$, $x = (1 - 16\zeta)^{1/4}$, $y = (1 - 16\zeta)^{1/2}$.

In addition, the RSL effect is taken into account in the Li scheme. The definition and influence of RSL will also be discussed in Sect. 4.1. De Ridder (2010) proposed the expression of ψ_M^* and ψ_H^* :

$$\psi_M^* \left(\zeta, \frac{z}{z_*} \right) = \phi_M \left[\left(1 + \frac{v}{\mu_M z / z_*} \right) \zeta \right] \frac{1}{\lambda} \ln \left(1 + \frac{\lambda}{\mu_M z / z_*} \right) e^{-\mu_M z / z_*}, \quad (10a)$$

$$\psi_H^* \left(\zeta, \frac{z}{z_*} \right) = \phi_H \left[\left(1 + \frac{v}{\mu_H z / z_*} \right) \zeta \right] \frac{1}{\lambda} \ln \left(1 + \frac{\lambda}{\mu_H z / z_*} \right) e^{-\mu_H z / z_*}, \quad (10b)$$

where $v = 0.5$, $\mu_M = 2.59$, $\mu_H = 0.95$, $z_* = 16.7 z_{om}$, $\lambda = 1.5$. ϕ_M and ϕ_H are universal functions before integration. Here, set $\chi_M = 1 + \frac{v}{\mu_M z / z_*}$, $\chi_H = 1 + \frac{v}{\mu_H z / z_*}$:

$$\phi_M(\chi_M \zeta) = 1 + a \frac{\chi_M \zeta + (\chi_M \zeta)^b \left[1 + (\chi_M \zeta)^b \right]^{\frac{1-b}{b}}}{\chi_M \zeta + \left[1 + (\chi_M \zeta)^b \right]^{\frac{1}{b}}}, \quad \zeta > 0 \text{ (stable)}, \quad (11a)$$

150

$$\phi_H(\chi_H \zeta) = 1 + c \frac{\chi_H \zeta + (\chi_H \zeta)^d [1 + (\chi_H \zeta)^d]^{\frac{1-d}{d}}}{\chi_H \zeta + [1 + (\chi_H \zeta)^d]^{\frac{1}{d}}}, \quad \zeta > 0 \text{ (stable)}, \quad (11b)$$

151

$$\phi_M(\chi_M \zeta) = (1 - 16\chi_M \zeta)^{-1/4}, \quad \zeta < 0 \text{ (unstable)}, \quad (12a)$$

152

$$\phi_H(\chi_H \zeta) = (1 - 16\chi_H \zeta)^{-1/2}, \quad \zeta < 0 \text{ (unstable)}. \quad (12b)$$

153 2.3 The MM5 scheme

154

155

156

157

158

The MM5 scheme is a classic one which is widely applied in modeling investigation (Hu et al., 2010; Wang et al., 2015a, b; Tymvios et al., 2017). This scheme does not distinguish z_{0h} from z_{0m} , thus the roughness length here is expressed as z_0 . For unstable conditions, the function forms are given by Eqs. (16a) and (16b) following Paulson (1970), and for stable conditions, the atmospheric stratification conditions are subdivided into three cases according to Zhang and Anthes (1982) and the function forms are given by Eqs. (13), (14), and (15).

159

(1) Strongly stable condition ($Ri_B \geq 0.2$):

160

$$\psi_M = \psi_H = -10 \ln \frac{z}{z_0}. \quad (13)$$

161

(2) Weakly stable condition ($0 < Ri_B < 0.2$):

162

$$\psi_M = \psi_H = -5 \left(\frac{Ri_B}{1.1 - 5 Ri_B} \right) \ln \frac{z}{z_0}. \quad (14)$$

163

(3) Neutral condition ($Ri_B = 0$):

164

$$\psi_M = \psi_H = 0. \quad (15)$$

165

(4) Unstable condition ($Ri_B < 0$):

166

$$\psi_M = 2 \ln \frac{1+x}{2} + \ln \frac{1+x^2}{2} - 2 \arctan(x) + \frac{\pi}{2}, \quad (16a)$$

167

$$\psi_H = 2 \ln \frac{1+y}{2}, \quad (16b)$$

168

where $x = (1 - 16\zeta)^{1/4}$, $y = (1 - 16\zeta)^{1/2}$.

169

170

171

172

This scheme calculates turbulent fluxes of the momentum and sensible heat with u_* and θ_* . In order to avoid the huge difference of u_* through between the two computations, u_* is arithmetically averaged with its previous value by Eq. (17), and a lower limit of $u_* = 0.1$ m/s is imposed to prevent the heat flux from being zero under very stable conditions. According to the profile functions of wind and temperature near the ground, θ_* is then deduced by Eq. (18).

173

$$u_* = \frac{1}{2} \left(u_* + \frac{ku}{\ln \frac{z}{z_{0m}} - \psi_M} \right), \quad (17)$$

174

$$\theta_* = \frac{k(\theta - \theta_g)}{R \left[\ln \frac{z}{z_{0h}} - \psi_H \right]}. \quad (18)$$

175

176

177

The calculation procedure of the Li scheme is the following: (1) determine Ri_B and z_{0h} according to the observation data; (2) calculate ζ with Ri_B and z_{0h} ; (3) calculate the momentum and sensible heat fluxes under different conditions. The MM5 scheme is summarized as follows: (1) determine the universal functions according to the values

178 of Ri_B and z_0 ; (2) calculate the u_* and θ_* with the meteorological variables and flux data; (3) derive the turbulent fluxes.
179 ~~Compared~~ Comparing with other non-iterative schemes including MM5, the Li scheme can be applied to the full range of
180 roughness status $10 \leq \frac{z}{z_{om}} \leq 10^5$ and $-0.5 \leq \ln \frac{z_{om}}{z_{oh}} \leq 30$ under whole conditions $-5 \leq Ri_B \leq 2.5$. In addition, there are
181 three obvious differences between the Li and MM5 schemes: (1) Li distinguishes z_{oh} from z_{om} but MM5 does not
182 ~~distinguish them~~; (2) the two schemes apply different universal functions under stable conditions; (3) Li considers the RSL
183 effect while MM5 ignores it.

184 3 Observational data and methods

185 The observational fluxes used in this study were measured at Gucheng station from December 1, 2016 to January 9, 2017.
186 Gucheng station (115.40 ° E, 39.08 ° N) is located at Gucheng County, Baoding, Hebei province and it is about 110km
187 southwest of Beijing (Fig. 1a). This station has a farmland site where rice is ~~planted~~ grown in summer and wheat in winter.
188 The surroundings are mainly farmland and scattered villages (Fig. 1b). At Gucheng station, the momentum and sensible heat
189 fluxes near the surface were measured by the eddy correlation flux measurement system. The system is mainly composed of a
190 sonic anemometer (CSAT3) and a gas analyzer (LI-7500). They are set up at 4 m height above the surface ground. The
191 measured fluxes are used to evaluate the two schemes as well as estimate the roughness lengths. The measured meteorological
192 variables including wind speed and direction, temperature, humidity, pressure, radiation are utilized to calculate the momentum
193 and sensible heat fluxes both in the Li and MM5 schemes. Note the observed meteorological data were from Gucheng station
194 and national basic automatic weather stations in Jing-Jin-Ji in eastern China, respectively. Hourly surface PM_{2.5} mass
195 concentration in Baoding and Beijing from China National Environmental Monitoring Centre (<http://www.cnemc.cn/>) was
196 also used in this paper.

197 3.1 Data processing

198 To obtain accurate flux data, quality control has been performed for the observational data, including: (1) eliminate the
199 outliers and the data in rainy days; (2) double rotation and WPL correction (Webb et al., 1980); (3) omit the dataset when the
200 wind speed is less than 0.5 m s⁻¹. In addition, the wind field especially the wind direction has a great impact on the value of
201 z_{om} , so it is necessary to understand the situation at Gucheng station. Figure 2 shows the distribution frequency of wind speed
202 and wind direction at Gucheng during the observation (December 1, 2016 ~ January 9, 2017). The wind speed is stable during
203 this period and the maximum is no more than 5 m s⁻¹ and most of them are about 1 ~ 2 m s⁻¹. The wind direction is relatively
204 uniform except for the southeast wind (135 °).

205 3.2 Determination of surface skin temperature

206 The surface skin temperature at Gucheng station is calculated from the radiation data by the following formula:

$$R_{lw}^{\uparrow} = (1 - \varepsilon_s)R_{lw}^{\downarrow} + \varepsilon_s\sigma T_g^4, \quad (19)$$

where R_{lw}^{\uparrow} and R_{lw}^{\downarrow} are the surface upward longwave radiation and long wave radiation incident on the surface, respectively. σ is the Stephen Boltzmann constant, $\sigma = 5.67 \times 10^{-8} \text{ W m}^{-2} \text{ K}^{-4}$. T_g is the surface skin temperature, ε_s is the surface emissivity which is the prerequisite ~~offer calculating~~ T_g calculation. Many researches estimated the value of ε_s and ~~found the range of the values~~ it is always 0.9 ~ 1 (Stewart et al., 1994; Verhoef et al., 1997). According to the semi-empirical method in Yang et al. (2008), ε_s is estimated when the RMSE is minimal. In this paper, the Li and MM5 schemes were used to estimate the ε_s value (as shown in Fig. 3). It is clear that the ε_s value corresponding to the minimum RMSE is not very sensitive to the choice of two schemes. When ε_s is 1, the RMSE has the minimum value. Thus, this experiment takes 1 as the optimal value of ε_s .

3.3 Determination of roughness length z_{0m} (z_{0h})

Using the observed momentum and sensible heat fluxes and the meteorological variables including wind speed, temperature, humidity and pressure after quality control at Gucheng station, z_{0m} and z_{0h} were derived from Eqs. (20a) and (20b) following Yang et al. (2003) and Sicart et al. (2014).

$$\frac{u_*}{u} = \frac{k}{\ln \frac{z}{z_{0m}} - \psi_M}, \quad (20a)$$

$$\frac{\theta_*}{(\theta - \theta_g)} = \frac{k}{R[\ln \frac{z}{z_{0h}} - \psi_H]}. \quad (20b)$$

During the observation period, the crops stopped growing and the height did not exceed 0.1 m, so the zero-plane displacement height was ignored ~~henceand~~ the reference height z was taken as 4m. The observation time was too short (about 1 month) to consider the effect of seasonal variations on the roughness lengths. Thus, z_{0m} and z_{0h} were assumed as two fixed values. Based on the variables and formulae mentioned above, the two roughness lengths at Gucheng are derived: $z_{0m} = 0.0419 \text{ m}$, $z_{0h} = 0.0042 \text{ m}$.

4 Results and discussion

The definitions and influences of RSL, roughness length ~~and their influence~~ on the calculation of turbulent flux are discussed in detail in this section. The Li and MM5 schemes are ~~offline~~ tested offline and evaluated during the haze pollution from December 13 to 23, 2016.

4.1 The influences of RSL and roughness length on the calculation of turbulent flux

The RSL is usually defined as the region where the flow is influenced by the individual roughness elements as reflected by the spatial inhomogeneity of the mean flow (Florens et al., 2013). In the RSL, turbulence is strongly affected by individual roughness elements, and the standard MOST is no longer valid (Simpson et al., 1998). Therefore, it is necessary to consider

235 the RSL effect in the calculation of turbulent flux, especially for the rough terrain such as forest or large cities. z_{0m} is defined
 236 as the height at which the extrapolated wind speed following the similarity theory vanishes. It is mainly determined by land-
 237 cover type and canopy height after excluding large obstructions. In models, z_{0m} is always based on the look-up table which
 238 is related to land-cover types. In this study, z_{0m} was simply classified based on the research of Stull (1988) and listed in
 239 Table 1. It can be seen in Table 1 that the rougher underlying surface corresponds to the larger value of z_{0m} . z_{0h} is the height
 240 at which the extrapolated air temperature is identical to the surface skin temperature. Some early researchers assumed that
 241 z_{0m} was equal to z_{0h} (Louis, 1979; Louis et al., 1982). However, the assumption is not applicable in reality because z_{0m}
 242 and z_{0h} have different physical meanings. Different treatments of z_{0m} and z_{0h} may introduce considerable changes in the
 243 surface flux calculation (Launiainen, 1995; Kot and Song, 1998; Anurose and Subrahmanyam, 2013). Many studies removed
 244 the assumption that z_{0m} was equal to z_{0h} and made the schemes more applicable in the situation that z_{0m} was not equal to
 245 z_{0h} or the ratio of z_{0m} to z_{0h} was much large (Wouters et al., 2012; Li et al., 2014; Li et al., 2015). Some field experiments
 246 even indicated the ratio z_{0m}/z_{0h} has a diurnal variation (Sun, 1999; Yang, 2003; Yang, 2008). In this study, we make the
 247 common assumption that the ratio z_{0m}/z_{0h} is a constant.

248 Considering the lowest level in mesoscale models is usually about 10m, $z = 10 \text{ m}$ is set as the reference height in this
 249 study. The range of Ri_B is set according to Louis82 (Louis et al., 1982) in the following discussion. Firstly, the study discusses
 250 the effects of different land-cover types (different z_{0m} values) and RSL on flux calculation were discussed. Set $z_{0m} = z_{0h}$,
 251 corresponding to four cases: $z_{0m} = 1, 0.5, 0.05, 0.001 \text{ m}$. These cases correspond to large cities, forests, agricultural fields and
 252 wide water surface, respectively. Figure 4 shows the relationship between $C_M(C_H)$ and Ri_B for under different z_{0m} values
 253 and treatments of RSL. It can be seen that both RSL and z_{0m} have impacts on C_M and C_H . Ignoring the RSL effect can
 254 results in larger C_M and C_H , compared-comparing with the results of original scheme considering the RSL effect. The
 255 difference induced by RSL effect is evident only under the rough surface. For example, the difference under $z_{0m} = 1$ is
 256 obviously greater than other z_{0m} settings, and when z_{0m} is reduced to 0.05 or less, the RSL has little effect. Furthermore,
 257 the RSL contributes more to sensible heat transfer than to momentum transfer under the same setting of z_{0m} . The effects of
 258 different land-cover types on C_M and C_H are much more significant compared-comparing with RSL. The rougher the surface
 259 is (corresponding to the larger z_{0m} value) brings, the larger the $C_M(C_H)$ is under the same stability. In addition, there is a
 260 corresponding relationship between $C_M(C_H)$ and stability. The more unstable the atmosphere is, the larger difference. The
 261 value of $C_M(C_H)$ drops is and vice versa with the stability. Once Ri_B exceeds the critical value (generally $0.2 \sim 0.25$), the
 262 transfer coefficients decline sharply but still above 0.

263 Secondly, the effects of difference between z_{0m} and z_{0h} as well as RSL on flux calculation are discussed. The
 264 relationship between z_{0m} and z_{0h} can be expressed as $kB^{-1} = \ln \frac{z_{0m}}{z_{0h}}$. Over the sea, z_{0m} is comparable to z_{0h} ; over the
 265 uniform vegetation surface (e.g., grassland, farmland, woodland), kB^{-1} is about 2 ($z_{0m}/z_{0h} \approx 10$) (Garratt and Hicks, 1973;

266 Garratt, 1978; Garratt and Francey, 1978), which coincides with our results in Gucheng ($z_{0m} = 0.0419$ m, $z_{0h} = 0.0042$ m);
267 over the surface with bluff roughness elements, the kB^{-1} value may be very large. For example, in some large cities, kB^{-1}
268 is even up to 30 ($z_{0m}/z_{0h} \approx 10^{13}$) (Sugawara and Narita, 2009). Therefore, the ratio z_{0m}/z_{0h} varies over a wide range.
269 Figure 5 shows the relationship between $C_M(C_H)$ and Ri_B ~~underfor~~ different treatments of z_{0m}/z_{0h} . Set $z_{0m} = 1$ as a large
270 city case, $z_{0h} = 1, 0.01, 10^{-4}, 10^{-6}$ m, and the large differences derived from the different ratios are displayed in Fig. 5. ~~The~~
271 ~~similar RSL effect can be found compared with Fig. 4.~~ The differences induced by RSL effect are more obvious than ~~thatose~~
272 in Fig. 4. The different treatments of ratio z_{0m}/z_{0h} ~~have~~ great impacts on turbulent flux transfer, particularly for sensible
273 heat transfer. It seems evident that when z_{0h} is not equal to z_{0m} ($z_{0m}/z_{0h} = 100 \sim 10^6$), the calculated C_H is much small
274 compared to the treatment that z_{0h} is equal to z_{0m} ($z_{0m}/z_{0h} = 1$). In addition, $C_M(C_H)$ decreases with the ~~increase of~~
275 stability, and ~~itthey~~ decreases much slower when z_{0h} is not equal to z_{0m} .
276

277 4.2 Comparison of momentum and sensible heat fluxes calculated by the two schemes

278 Using the obtained roughness lengths and the observations, the momentum and sensible heat flux were calculated by the
279 Li and MM5 schemes. Firstly, z_{0m} and z_{0h} were set as 0.0419 and 0.0042 respectively in the Li scheme, z_0 was equal to
280 z_{0m} in the MM5 scheme to calculate the momentum and sensible heat fluxes and the results are shown in Figs. 6a and 6b. It
281 can be seen that ~~compared comparing~~ with MM5, Li performs better with higher regression coefficient and determination
282 coefficient. For the momentum fluxes, the regression coefficient by Li is 0.6795 and that by MM5 is 0.5598, indicating that
283 the error of Li is 12 % lower than that of MM5. For sensible heat fluxes, the regression coefficient by Li is 0.7967 and that by
284 MM5 is 1.7994. The latter is much larger than 1, that is, the MM5 scheme obviously overestimates the sensible heat due to it
285 does not distinguish z_{0h} from z_{0m} . Then, make z_0 equal to 0.0042 in the MM5 scheme to re-calculate the sensible heat
286 fluxes ~~and the result is as~~ shown in Fig. 6c. It can be seen the result has a great improvement after modifying z_0 value and the
287 regression coefficient by MM5 is 0.7363, indicating that the error was reduced by 54 % after considering the z_{0h} effect. The
288 result indicates that z_{0h} plays a critical role in both the SL scheme and the sensible heat flux (Chen and Zhang, 2009; Chen
289 et al., 2011). However, the error ~~caused by Li of MM5~~ is still 6 % ~~lowerlarger~~ than that ~~by of MM5 Li~~. This illustrates that in
290 addition to the effect of roughness lengths, the algorithm of the Li scheme itself is more reasonable than that of MM5 scheme.

291 4.3 The specific performance of the two schemes in the severe haze pollution

292 There were two obvious pollution processes during this observation period and one occurred during December 13 to 23,
293 2016. Figure 7 shows the variations of hourly observed $PM_{2.5}$ concentration as well as the momentum and sensible heat fluxes
294 calculated by the Li and MM5 schemes at Gucheng station in this process. For the research purpose significance, only the
295 daytime (from 8:00 a.m. to 20:00 p.m.) was taken into account. Note in MM5, z_0 was 0.0419 when calculate momentum

296 fluxes and it was 0.0042 when calculate sensible heat fluxes. As shown in Fig. 7, the calculated results of momentum and
297 sensible heat fluxes ~~for~~by the two schemes are generally consistent with the trend of the observations. Specifically, for the
298 momentum fluxes (Fig. 7a), the results of two schemes have little difference when the values of observed momentum fluxes
299 are large or at the peak. When the observed momentum fluxes are small, ~~the Li-scheme~~ results are close to or less than the
300 observations, while ~~the MM5-scheme~~ results are always higher than observations because of the limit of $u_* = 0.1$ in this
301 scheme. For the sensible heat fluxes (Fig. 7b), MM5 results are always lower while Li results are closer to observations
302 especially when the observed values are small. Furthermore, according to the evolution of PM_{2.5} concentration, this haze event
303 was then divided into three stages: the clear stage (stage 1: 13~14), the transition stage (stage 2: 16~18) and the maintenance
304 stage (stage 3: 21~22). As shown in Fig. 7, in the clear stage (stage 1), the atmospheric stratification is unstable, PM_{2.5}
305 concentration is low and there is a strong flux transport in the SL, the corresponding observations of the momentum and
306 sensible heat fluxes are relatively high and they vary greatly. In the transition stage (stage 2), the atmosphere is changing from
307 unstable to stable corresponding to haze formation, the momentum and sensible heat fluxes gradually decrease and the daily
308 variation also decreases. In the maintenance stage (stage 3), the atmospheric stratification is very stable, and flux transport in
309 the SL is weak, both the momentum and sensible heat fluxes are at a low level. It can be seen that the Li results are generally
310 closer to the observations ~~compared~~comparing with MM5 results in all three stages.

311 Figure 8 shows the probability distribution functions (PDF) of the difference ~~between calculated fluxes (by using the Li~~
312 ~~and MM5 schemes) and observations in different stages at Gucheng station. of momentum fluxes (Figs. 8a, 8c, 8e, 8g) and~~
313 ~~sensible heat fluxes (Figs. 8b, 8d, 8f, 8h) calculated by using the Li and MM5 schemes in different stages at Gucheng station.~~
314 In the whole pollution process, for the momentum fluxes (Fig. 8a), the PDF ~~of the difference by~~from Li tends to cluster in a
315 narrower range centered by 0, and the probability within $\pm 0.005 \text{ N m}^{-2}$ is 46.82 %, while this value ~~by~~from MM5 falls to
316 23.02 %. For the sensible heat fluxes (Fig. 8b), the PDF ~~of the difference by~~from Li is also more concentrated around 0 than
317 that ~~by~~from MM5. The probabilities of bias ~~from~~by Li and MM5 within $\pm 2.5 \text{ W m}^{-2}$ are 32.54 % and 13.49 %, respectively. In
318 stage 1, for the momentum fluxes (Fig. 8c), the probability of bias ~~by~~from Li within $\pm 0.005 \text{ N m}^{-2}$ is 38.09 %. The bias ~~from~~of
319 MM5 mainly concentrates larger than 0, and the probability within $\pm 0.005 \text{ N m}^{-2}$ is 14.29 %. For the sensible heat fluxes (Fig.
320 8d), the probability of Li-bias ~~from~~Li within $\pm 2.5 \text{ W m}^{-2}$ is 38.09 %, the same as momentum fluxes. The bias ~~from~~of MM5
321 mainly concentrates less than 0, and the probability within $\pm 2.5 \text{ W m}^{-2}$ is 9.52 %. In stage 2, the differences between the two
322 schemes are more obvious. The ~~PDFs momentum and sensible heat fluxes bias by~~from Li ~~is~~ are the most concentrated around
323 0 in all cases, while ~~the distribution of bias by~~those from MM5 ~~are~~ is similar to ~~that in~~stage 1. Specifically, for the momentum
324 fluxes (Fig. 8e), the probabilities of bias ~~by~~from Li and MM5 within $\pm 0.005 \text{ N m}^{-2}$ are 56.25 % and 25.00 %. For the sensible
325 heat fluxes (Fig. 8f), the ~~values probabilities of bias by~~Li and MM5 within $\pm 2.5 \text{ W m}^{-2}$ are 40.62 % and 6.25 %. In stage 3, the
326 difference between two schemes is small. For the momentum fluxes (Fig. 8g), the probabilities of bias ~~by~~from Li and MM5

327 within $\pm 0.005 \text{ N m}^{-2}$ are 22.73 % and 27.27 %. For the sensible heat fluxes (Fig. 8h), the ~~values probabilities of bias by from~~ Li
328 and MM5 within $\pm 2.5 \text{ W m}^{-2}$ are both 36.36 %.

329 Mean bias (MB), normalized mean bias (NMB), normalized mean error (NME) and root mean square error (RMES) ~~of~~
330 ~~Li and MM5~~ were calculated to test the results of two schemes. Table 2 shows that the Li scheme generally estimates better
331 than the MM5 scheme. In the whole haze process, the Li scheme underestimates the momentum fluxes by 3.63 % relative to
332 the observations, while the MM5 scheme overestimates by 34.03 %. The Li and MM5 schemes underestimate the sensible heat
333 fluxes by 15.69 % and 50.22 %, respectively. In the three stages, the Li scheme performs much better than the MM5 scheme
334 in the stage 1 and stage 2, especially in stage 2 when atmospheric stratification transforms from unstable to stable condition,
335 the difference between the Li and MM5 schemes ~~are is~~ particularly significant. ~~That is, T~~the Li and MM5 schemes overestimate
336 the momentum fluxes by 7.68% and 45.56 %, respectively, ~~while and Li and MM5 they~~ underestimate the sensible heat fluxes
337 by 33.84 % and 76.88 %. The error of Li is much less than that of MM5. ~~Considering In view of~~ the importance role of
338 atmospheric stratification in the generation and accumulation of $\text{PM}_{2.5}$ in stage 2, the Li scheme is expected to show better
339 performance in online simulation of $\text{PM}_{2.5}$ than MM5.

340 Based on the good behavior of the Li scheme in Gucheng, the same experiment was performed at Beijing station to discuss
341 the effect of different land-cover types on flux calculation ~~for two schemes~~. For Beijing station, the assumption $z_{0m} = 1 \text{ m}$,
342 $z_{0m}/z_{0h} = 10^6$ was made to represent the surface condition of megacity due to a lack in situ measurements of surface
343 turbulent flux. As shown in Fig. 9, the evolution of $\text{PM}_{2.5}$ concentration at Beijing station was also divided into three stages
344 (stage 1: 13~15; stage 2: 17~19; stage 3: 20~21) ~~just like Gucheng shown in Fig. 7 in the discussion~~. ~~Compareing with Gucheng~~
345 ~~to Fig. 7, there is a significant increase in the difference of momentum and sensible heat fluxes between Li and MM5 in Fig.~~
346 ~~9. To be specific,~~ the momentum transfer in at Beijing station is obviously larger ~~than that in Gucheng~~ due to the great increase
347 of the urban aerodynamic roughness length (z_{0m}). In the meanwhile, the difference between Li and MM5 has a further
348 expansion at Beijing station ~~compared with Gucheng~~. The sensible heat transfer ~~by of~~ the Li scheme has great difference
349 between clear days and pollution days, which is, the sensible heat transfer changes acutely in the stage 1 while it changes
350 smoothly in the stage 2 and stage 3. ~~However, T~~the result sensible heat transfer by of the MM5 scheme is significantly different
351 ~~compared from with~~ Li result due to MM5 ignore ~~sd~~ the z_{0m} effect, and the small number of z_{0h} keeps the sensible heat
352 fluxes at a low level in all three stages.

353 To quantify the differences ~~s~~ between the two schemes, a relative difference is defined in percentage:

$$354 \quad \Delta V = \left| \frac{V_{\text{Li}} - V_{\text{MM5}}}{V_{\text{MM5}}} \right| \times 100 \%, \quad (21)$$

355 where V_{Li} and V_{MM5} are the momentum (or sensible heat) fluxes calculated by the Li and MM5 schemes, respectively. We
356 obtained the relative differences at the two stations in the three stages through the statistics. It is clearly that the larg est relative
357 difference at Gucheng station is in the stage 2 and ~~the value that~~ at Beijing station is in the stage 1. The differences in Beijing

358 are always larger than those at in Gucheng for each three stages. Specifically, the relative differences of momentum flux in
359 stage 1, stage 2 and stage 3 increases by 73 %, 34 % and 27 %, respectively, and the results of sensible heat flux are 289 %,
360 52 % and 68 %, respectively.

361 We further estimated the surface fluxes tested the two schemes in whole Jing-Jin-Ji region by using the two schemes.
362 Figure 10 shows the mean momentum and sensible heat fluxes calculated by Li and MM5 schemes and their differences in
363 Jing-Jin-Ji during the pollution episode. The assumption ($z_{0m} = 0.1 \text{ m}$, $z_{0m}/z_{0h} = 10^3$) were was used to represent the
364 average condition of the underlying surface of Jing-Jin-Ji region. As shown in Fig. 10, the momentum fluxes calculated by Li
365 are less than that those by MM5 in most stations; the sensible heat fluxes calculated by Li are usually larger than that those by
366 MM5. The result is consistent with the experiment of at Gucheng station, which further indicates the importance of considering
367 both z_{0m} and z_{0h} at the same time.

368 5 Conclusions

369 Using the observed momentum and sensible heat fluxes, together with conventional meteorological data including
370 pressure, temperature, humidity and wind speed from December 1, 2016 to January 9, 2017, including a severe pollution
371 episode from December 13 to 23, 2016, the differences and the performance of between the Li and MM5 schemes two surface
372 schemes and the specific performances of the two were discussed and evaluated in this paper. The evolution process of
373 atmospheric stratification from unstable to stable corresponding to $\text{PM}_{2.5}$ accumulation increasing was mainly discussed. The
374 contributions of roughness lengths (z_{0m} and z_{0h}) as well as other factors in the SL schemes to the momentum and sensible
375 heat flux flux calculation for the momentum and sensible heat were also discussed in details. The results are summarized as
376 follows:

377 1) z_{0m} and z_{0h} have important effects on turbulent flux calculation in the SL schemes. Different values of z_{0m} and
378 z_{0h} in the schemes could induce great changes in the flux calculation, indicating that it is very necessary and important to
379 distinguish z_{0h} from z_{0m} . Ignoring the difference between the two in the MM5 scheme led to large errors in the calculation
380 of sensible heat fluxes and this error in Gucheng was 54 %. Besides the roughness lengths, the algorithms of two in schemes
381 are also one of the important factors. In addition, ignoring the effect of the RSL in schemes may also result in certain bias of
382 momentum and sensible heat fluxes in megacity regions which represent the rough underlying surface.

383 2) The effect of z_{0m}/z_{0h} on turbulent fluxes is closely related to land-cover types (z_{0m}). A rough land-cover type (large
384 z_{0m}) should be accompanied by a large value of z_{0m}/z_{0h} . The differences between the two schemes for of the momentum and
385 sensible heat fluxes calculated by Li and MM5 in Beijing were much larger bigger in Beijing than that those in Gucheng. This
386 suggests that the MM5 scheme probably induces bigger greater error in megacities with rough surface (e.g., Beijing) than it in

suburban areas with smooth surface (e.g., Gucheng) due to the irrational algorithm of MM5 scheme itself and the ignoring difference between z_{0m} and z_{0h} .

3) The Li scheme generally performed better than the MM5 scheme in the calculation of both the momentum flux and the sensible heat flux ~~compared with observations~~ at Gucheng station. The Li scheme made a better description in atmospheric stratification which is closely related to the haze pollution, ~~compared~~ ~~comparing~~ with the MM5 scheme. This advantage was the most prominent in the transition stage from unstable to stable atmospheric stratification corresponding to the PM_{2.5} accumulation. In this stage, the momentum flux calculated by Li was overestimated by 7.68 % and this overestimation by MM5 was up to 45.56 %; the sensible heat flux by Li was underestimated by 33.84 % while this underestimation by MM5 was even up to 76.88 %. In most Jing-Jin-Ji region, the momentum fluxes calculated by Li were less than ~~th~~~~ose~~ by MM5 and the sensible heat fluxes by Li were larger than ~~th~~~~ose~~ by MM5, which ~~was~~ ~~were~~ consistent with Gucheng.

The offline study of the two SL schemes in this paper showed the superiority of the Li scheme for surface flux calculation corresponding to the PM_{2.5} evolution during the haze episode in Jing-Jin-Ji in eastern China. The study results offer the prerequisite and a possible way to improve PBL diffusion simulation and then PM_{2.5} prediction, which will be achieved in the follow-up work of ~~online~~ integrating ~~of~~ the Li scheme into ~~the~~ atmosphere chemical models.

Author contributions

HW and YP conducted the study design. YL and CL provided the Li scheme and the flux data. CL helped with data processing. YP wrote the manuscript with help of HW and TZ. XZ, ZG, TJ, HC and MZ were involved in the scientific interpretation and discussion. All the authors commented on the paper.

Acknowledgments

The study was supported by the National Key Project (2016YFC0203306, 2016YFC0203304), the National (Key) Basic Research and Development (973) Program of China (2014CB441201), the National Natural Science Foundation of China (41505004, 41675009), and Jiangsu Provincial Natural Science Fund Project (BK20150910).

References

- Anurose, T. J., and Subrahmanyam, D. B.: Improvements in Sensible Heat-Flux Parametrization in the High-Resolution Regional Model (HRM) Through the Modified Treatment of the Roughness Length for Heat, Bound.-Lay. Meteorol., 147, 569-578, <https://doi.org/10.1007/s10546-013-9799-9>, 2013.
- Ban, J., Gao, Z., and Lenschow, D. H.: Climate simulations with a new air-sea turbulent flux parameterization in the National Center for Atmospheric Research Community Atmosphere Model (CAM3), J. Geophys. Res.-Atmos., 115, <https://doi.org/10.1029/2009JD012802>, 2010.

416 Beljaars, A. C. M., and Holtslag, A. A. M.: Flux parameterization over land surfaces for atmospheric models, *J. Appl.*
417 *Meteor.*, 30, 327-341, 1991.

418 Businger, J. A., Wyngaard, J. C., Izumi, Y., and Bradley, E. F.: Flux-profile relationships in the atmospheric surface layer, *J.*
419 *Atmos. Sci.*, 28, 181-189, 1971.

420 Businger, J. A.: Transfer of momentum and heat in the planetary boundary layer, *Proc. Symp. Arctic Heat Budget and*
421 *Atmospheric Circulation*, RM-5233-NSF, 305-331, 1966.

422 Chen, F., and Zhang, Y.: On the coupling strength between the land surface and the atmosphere: From viewpoint of surface
423 exchange coefficients, *Geophys. Res. Lett.*, 36, <https://doi.org/10.1029/2009GL037980>, 2009.

424 Chen, Y., Yang, K., He, J., Qin, J., Shi, J., Du, J., and He, Q.: Improving land surface temperature modeling for dry land of
425 China, *J. Geophys. Res.-Atmos.*, 116, <https://doi.org/10.1029/2011JD015921>, 2011.

426 Cheng, F. Y., Chin, S. C., and Liu, T. H.: The role of boundary layer schemes in meteorological and air quality simulations of
427 the Taiwan area, *Atmos. Environ.*, 54, 714-727, <https://doi.org/10.1016/j.atmosenv.2012.01.029>, 2012.

428 Cheng, Y., and Brutsaert, W.: Flux-profile relationships for wind speed and temperature in the stable atmospheric boundary
429 layer, *Bound.-Lay. Meteorol.*, 114, 519-538, <https://doi.org/10.1007/s10546-004-1425-4>, 2005.

430 De Ridder, K.: Bulk Transfer Relations for the Roughness Sublayer, *Bound.-Lay. Meteorol.*, 134, 257-267,
431 <https://doi.org/10.1007/s10546-009-9450-y>, 2010.

432 Dyer, A. J.: A review of flux-profile relationships, *Bound.-Lay. Meteorol.*, 7, 363-372, <https://doi.org/10.1007/BF00240838>,
433 1974.

434 Dyer, A. J.: The turbulent transport of heat and water vapour in an unstable atmosphere, *Quart. J. Roy. Meteor. Soc.*, 93, 501-
435 508, <https://doi.org/10.1002/qj.49709339809>, 1967.

436 Florens, E., Eiff, O., and Moulin, F.: Defining the roughness sublayer and its turbulence statistics, *Exp. Fluids*, 54, 1500,
437 <https://doi.org/10.1007/s00348-013-1500-z>, 2013.

438 Garratt, J. R., and Francey, R. J.: Bulk characteristics of heat transfer in the unstable, baroclinic atmospheric boundary layer,
439 *Bound.-Lay. Meteorol.*, 15, 399-421, <https://doi.org/10.1007/BF00120603>, 1978.

440 Garratt, J. R., and Hicks, B. B.: Momentum, heat and water vapour transfer to and from natural and artificial surfaces, *Quart.*
441 *J. Roy. Meteor. Soc.*, 99, 680-687, 1973.

442 Garratt, J. R.: Transfer characteristics for a heterogeneous surface of large aerodynamic roughness, *Quart. J. Roy. Meteor.*
443 *Soc.*, 104, 491-502, 1978.

444 Högström, U.: Review of some basic characteristics of the atmospheric surface layer, *Bound.-Lay. Meteorol.*, 78, 215-246,
445 <https://doi.org/10.1007/BF00120937>, 1996.

446 Holtslag, A. A. M., and De Bruin, H. A. R.: Applied modeling of the nighttime surface energy balance over land, *J. Appl.*
447 *Meteor.*, 27, 689-704, 1988.

448 Hu, X. M., Nielsen-Gammon, J. W., and Zhang, F.: Evaluation of three planetary boundary layer schemes in the WRF model,
449 *J. Appl. Meteorol. Climatol.*, 49, 1831-1844, <https://doi.org/10.1175/2010JAMC2432.1>, 2010.

450 Jiménez, P. A., Dudhia, J., González-Rouco, J. F., Navarro, J., Montávez, J. P., and García-Bustamante, E.: A revised scheme
451 for the WRF surface layer formulation, *Mon. Wea. Rev.*, 140, 898-918, <https://doi.org/10.1175/MWR-D-11-00056.1>,
452 2012.

453 Kot, S. C., and Song, Y.: An Improvement of the Louis Scheme for the Surface Layer in an Atmospheric Modelling System,
454 *Bound.-Lay. Meteorol.*, 88, 239-254, <https://doi.org/10.1023/A:100119329423>, 1998.

455 Launiainen, J.: Derivation of the relationship between the Obukhov stability parameter and the bulk Richardson number for
456 flux-profile studie, *Bound.-Lay. Meteorol.*, 76, 165-179, <https://doi.org/10.1007/BF00710895>, 1995.

457 Li, T., Wang, H., Zhao, T., Xue, M., Wang, Y., Che, H., and Jiang, C.: The Impacts of Different PBL Schemes on the
458 Simulation of PM_{2.5} during Severe Haze Episodes in the Jing-Jin-Ji Region and Its Surroundings in China, *Adu.*
459 *Meteorol.*, <http://dx.doi.org/10.1155/2016/6295878>, 2016a.

460 Li, Y., Gao, Z., Li, D., Chen, F., Yang, Y., and Sun, L.: An Update of Non-iterative Solutions for Surface Fluxes Under
461 Unstable Conditions, *Bound.-lay. Meteorol.*, 156, 501-511, <https://doi.org/10.1007/s10546-015-0032-x>, 2015.

462 Li, Y., Gao, Z., Li, D., Chen, F., Yang, Y., and Sun, L.: Erratum to: An Update of Non-iterative Solutions for Surface Fluxes
463 Under Unstable Conditions, *Bound.-Lay. Meteorol.*, 161: 225-228, 2016b.

464 Li, Y., Gao, Z., Li, D., Wang, L., and Wang, H.: An improved non-iterative surface layer flux scheme for atmospheric stable
465 stratification conditions, *Geosci. Model Dev.*, 7, 515-529, <https://doi.org/10.5194/gmd-7-515-2014>, 2014.

466 Li, Y.: On the Surface Turbulent Fluxes Calculation in Numerical Models, Beijing: university of Chinese academy of
467 sciences, 2014.

468 Li, Z., Guo, J., Ding, A., Liao, H., Liu, J., Sun, Y., Wang, T., Xue, H., Zhang, H., and Zhu, B.: Aerosol and boundary-layer
469 interactions and impact on air quality, *Natl. Sci. Rev.*, 4, 810–833, <https://doi.org/10.1093/nsr/nwx117>, 2017.

470 Liu, T. T., Gong, S. L., He, J. J., Yu, M., Wang, Q. F., Li, H. R., Liu, W., Zhang, J., Li, L., Wang, X. G., Li, S. L., Lu, Y. L.,
471 Du, H. T., Wang, Y. Q., Zhou, C. H., Liu, H. L. and Zhao, Q. C.: Attributions of meteorological and emission factors to
472 the 2015 winter severe haze pollution episodes in China's Jing-Jin-Ji area, *Atmos. Chem. Phys.*, 17, 2971–2980,
473 <https://doi.org/10.5194/acp-17-2971-2017>, 2017.

474 Louis, J. F.: A parametric model of vertical eddy fluxes in the atmosphere. *Bound.-Lay. Meteorol.*, 17, 187-202,
475 <https://doi.org/10.1007/BF00117978>, 1979.

476 Louis, J. F., Tiedtke, M., and Geleyn, J. F.: A short history of the operational PBL parameterization at ECMWF, in Workshop
477 on Planetary Boundary Layer Parameterization, November 1981, ECMWF, Reading, U.K., pp. 59–79, 1982.

478 Monin, A. S., and Obukhov, A. M.: Basic laws of turbulent mixing in the surface layer of the atmosphere, *Contrib. Geophys.*
479 *Inst. Acad. Sci., USSR*, 24, 163–187, 1954.

480 Paulson, C. A.: The mathematical representation of wind speed and temperature profiles in the unstable atmospheric surface
481 layer, *J. Appl. Meteorol.*, 9, 857-861, 1970.

482 Sharan, M., and Srivastava, P.: A Semi-Analytical Approach for Parametrization of the Obukhov Stability Parameter in the
483 Unstable Atmospheric Surface Layer, *Bound.-Lay. Meteorol.*, 153, 339-353, [https://doi.org/10.1007/s10546-014-9948-](https://doi.org/10.1007/s10546-014-9948-9)
484 9, 2014.

485 Sicart, J. E., Litt, M., Helgason, W., Tahar, V. B., and Chaperon, T.: A study of the atmospheric surface layer and roughness
486 lengths on the high-altitude tropical Zongo glacier, Bolivia, *J. Geophys. Res.-Atmos.*, 119, 3793–3808,
487 <https://doi.org/10.1002/2013JD020615>, 2014.

488 Simpson, I. J., Thurtell, G. W., Neumann, H. H., Den Hartog, G., and Edwards, G. C.: The Validity of Similarity Theory in
489 the Roughness Sublayer Above Forests, *Bound.-Lay. Meteorol.*, 87, 69-99, <https://doi.org/10.1023/A:1000809902980>,
490 1998.

491 Stewart, J. B., Kustas, W. P., Humes, K. S., Nichols, W. D., Moran, M. S., and De Bruin, H. A. R.: Sensible heat flux-
492 radiometric surface temperature relationship for eight semiarid areas, *J. Appl. Meteorol.*, 33, 1110-1117, 1994.

493 Stull, R. B.: *An Introduction to Boundary Layer Meteorology*, Kluwer Academic Publishers, London, 1988.

494 Sugawara, H., and Narita, K.: Roughness length for heat over an urban canopy, *Theor. Appl. Climatol.*, 95, 291-299,
495 <https://doi.org/10.1007/s00704-008-0007-7>, 2009.

496 Sun, J.: Diurnal Variations of Thermal Roughness Height over a Grassland, *Bound.-Lay. Meteorol.*, 92, 407-427,
497 <https://doi.org/10.1023/A:1002071421362>, 1999.

498 Tymvios, F., Charalambous, D., Michaelides, S., and Lelieveld, J.: Intercomparison of boundary layer parameterizations for
499 summer conditions in the eastern Mediterranean island of Cyprus using the WRF-ARW model, *Atmos. Res.*, 208, 45-
500 59, <https://doi.org/10.1016/j.atmosres.2017.09.011>, 2017.

501 Vautard, R., Moran, M. D., Solazzo, E., Gilliam, R. C., Matthias, V., Bianconi, R., Chemel, C., Ferreira, J., Geyer, B.,
502 Hansen, A. B., Jericevic, A., Prank, M., Segers, A., Silver, J. D., Werhahn, J., Eolke, R., Rao, S. T., and Galmarini, S.:
503 Evaluation of the meteorological forcing used for the Air Quality Model Evaluation International Initiative (AQMEII)
504 air quality simulations, *Atmos. Environ.*, 53, 15-37, <https://doi.org/10.1016/j.atmosenv.2011.10.065>, 2012.

505 Verhoef, A., De Bruin, H. A. R., and Van Den Hurk, B. J. J. M.: Some Practical Notes on the Parameter kB-1 for Sparse
506 Vegetation., *J. Appl. Meteorol.*, 36, 560-572, 1997.

507 Wang, H., Shi, G. Y., Zhang, X. Y., Gong, S. L., Tan, S. C., Chen, B., Che, H. Z., and Li, T.: Mesoscale modeling study of the
508 interactions between aerosols and PBL meteorology during a haze episode in China Jing-Jin-Ji and its near surrounding
509 region - Part 2: Aerosols' radiative feedback effects, *Atmos. Chem. Phys.*, 15, 3277-3287, [https://doi.org/10.5194/acp-](https://doi.org/10.5194/acp-15-3277-2015)
510 15-3277-2015, 2015b.

511 Wang, H., Tan, S. C., Wang, Y., Jiang, C., Shi, G., Zhang, M., and Che, H. Z.: A multisource observation study of the severe
512 prolonged regional haze episode over eastern China in January 2013, *Atmos. Environ.*, 89, 807-815,
513 <https://doi.org/10.1016/j.atmosenv.2014.03.004>, 2014.

514 Wang, H., Xue, M., Zhang, X. Y., Liu, H. L., Zhou, C. H., Tan, S. C., Che, H. Z., Chen, B., and Li, T.: Mesoscale modeling
515 study of the interactions between aerosols and PBL meteorology during a haze episode in China Jing-Jin-Ji and its
516 nearby surrounding region - Part 1: Aerosol distributions and meteorological features, *Atmos. Chem. Phys.*, 15, 3257-
517 3275, <https://doi.org/10.5194/acp-15-3257-2015>, 2015a.

518 Wang, S., Wang, Q., and Doyle, J.: Some improvements to Louis surface flux parameterization. Paper presented at 15th
519 symposium on boundary layers and turbulence, American Meteorological Society, 15-19, 2002, Wageningen,
520 Netherlands.

521 Webb, E. K., Pearman, G. I., and Leuning, R.: Correction of flux measurements for density effects due to heat and water
522 vapour transfer, *Quart. J. Roy. Meteor. Soc.*, 106, 85-100, 1980.

523 Webb, E. K.: Profile relationships: The log-linear range, and extension to strong stability, *Quart. J. Roy. Meteor. Soc.*, 96, 67-
524 90, 1970.

525 Wouters, H., De Ridder, K., and van Lipzig, N. P. M.: Comprehensive Parametrization of Surface-Layer Transfer
526 Coefficients for Use in Atmospheric Numerical Models, *Bound.-Lay. Meteorol.*, 145, 539-550,
527 <https://doi.org/10.1007/s10546-012-9744-3>, 2012.

528 Xie, B., Fung, J. C. H., Chan, A., and Lau, A.: Evaluation of nonlocal and local planetary boundary layer schemes in the
529 WRF model, *J. Geophys. Res.-Atmos.*, 117, 48-50, <https://doi.org/10.1029/2011JD017080>, 2012.

530 Yang, K., Koike, T., and Yang, D.: Surface Flux Parameterization in the Tibetan Plateau, *Bound.-Lay. Meteorol.*, 106, 245-
531 262, <https://doi.org/10.1023/A:1021152407334>, 2003.

532 Yang, K., Koike, T., Ishikawa, H., Kim, J., Li, X., Liu, H., Liu, S., Ma, Y., and Wang, J.: Turbulent Flux Transfer over Bare-
533 Soil Surfaces: Characteristics and Parameterization, *J. Appl. Meteorol. Clim.*, 47, 276-290,
534 <https://doi.org/10.1175/2007jamc1547.1>, 2008.

535 Yang, K., Tamai, N., and Koike, T.: Analytical Solution of Surface Layer Similarity Equations, *J. Appl. Meteorol.*, 40, 1647-
536 1653, 2001.

537 Yang, Y., Liu, X., Qu, Y., Wang, J., An, J., Zhang, Y., and Zhang, F.: Formation mechanism of continuous extreme haze
538 episodes in the megacity Beijing, China, in January 2013, *Atmos. Res.*, 155, 192–203,
539 <https://doi.org/10.1016/j.atmosres.2014.11.023>, 2015.

540 Zhang, B., Wang, Y., and Hao, J.: Simulating aerosol-radiationcloud feedbacks on meteorology and air quality over eastern
541 China under severe haze conditionsin winter, *Atmos. Chem. Phys.*, 15, 2387–2404, <http://doi.org/10.5194/acp-15-2387->
542 2015, 2015.

543 Zhang, D., and Anthes, R. A.: A high-resolution model of the planetary boundary layer—Sensitivity tests and comparisons
544 with SESAME-79 data, *J. Appl. Meteorol.*, 21, 1594-1609, 1982.

545 Zhang, R., Li, Q., and Zhang, R.: Meteorological conditions for the persistent severe fog and haze event over eastern China
546 in January 2013, *Sci. China Earth Sci.*, 57, 26–35, <https://doi.org/10.1007/s11430-013-4774-3>, 2014.

547 Zhong, J., Zhang, X., Dong, Y., Wang, Y., Liu, C., Wang, J., Zhang, Y., and Che, H.: Feedback effects of boundary-layer
548 meteorological factors on cumulative explosive growth of PM_{2.5} during winter heavy pollution episodes in Beijing
549 from 2013 to 2016, *Atmos. Chem. Phys.*, 18, 247–258, <https://doi.org/10.5194/acp-18-247-2018>, 2018.

550

551 **Table 1.** Typical values of z_{0m} corresponding to various land-cover types

z_{0m} / m	Land-cover types
5 ~ 50	Mountain (above 100m)
1 ~ 5	The center of large cities, hills or mountain area
0.1 ~ 1	Forests, the center of large towns
0.01 ~ 0.1	Flat grasslands, agricultural fields
10^{-4} ~ 10^{-3}	The snow surface, wide water surface, flat deserts
10^{-5}	The ice surface

552

553

554

555

Table 2. Statistics between the Li and MM5 schemes calculated turbulent flux at Gucheng station.

		Li				MM5			
		MB	NMB	NME	RMSE	MB	NMB	NME	RMSE
Whole process	τ	-0.0006	-3.63 %	54.29 %	0.0142	0.0058	34.03 %	63.59 %	0.0143
	H	-2.2723	-15.69 %	52.73 %	10.9649	-7.2735	-50.22 %	69.68 %	12.7946
Stage 1	τ	0.0021	9.98 %	55.90 %	0.0172	0.0091	43.45 %	66.66 %	0.0169
	H	1.1775	5.79 %	37.87 %	10.5734	-7.1891	-35.34 %	55.70 %	13.1324
Stage 2	τ	0.0013	7.68 %	44.50 %	0.0111	0.0079	45.56 %	56.81 %	0.0121
	H	-4.5752	-33.84 %	50.28 %	9.3995	-10.3924	-76.88 %	81.40 %	13.2553
Stage 3	τ	-0.0024	-13.25 %	59.13 %	0.0144	0.0030	16.72 %	56.34 %	0.0138
	H	1.2818	11.39 %	66.31 %	11.4778	-1.7479	-15.52 %	65.90 %	10.4219

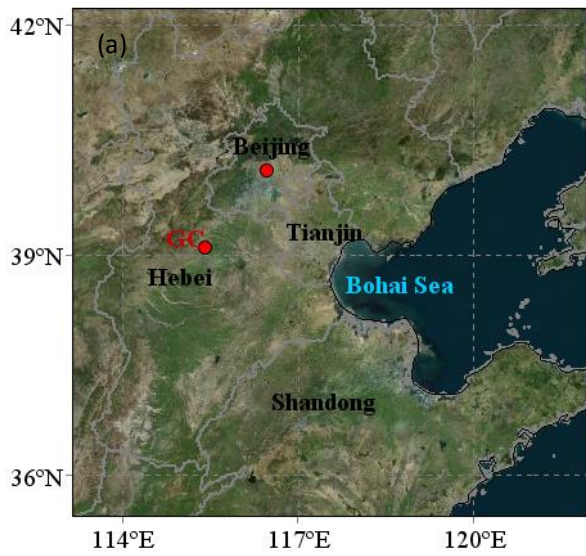
556

* τ : momentum flux; H: sensible heat flux; MB: mean bias; NMB: normalized mean bias; NME: normalized mean error;

557

RMSE: root mean square error. The units of MB and RMSE: $\mu\text{g m}^{-3}$.

558



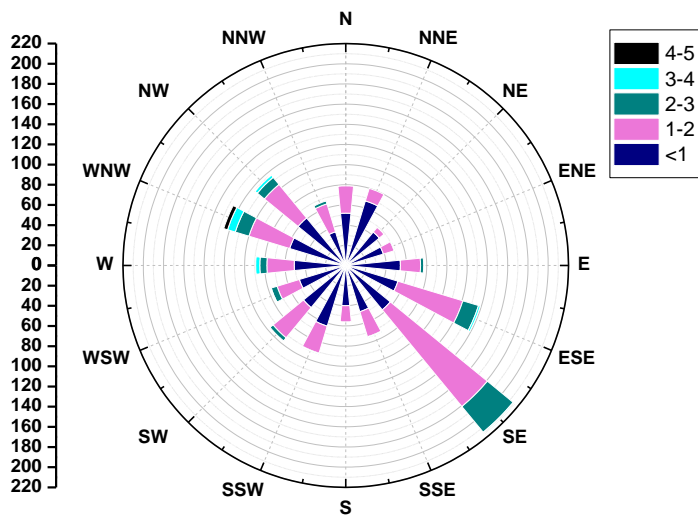
559

560 **Figure 1.** Location (a) and geographical environment (b) at Gucheng station. The map is from Bing Maps.

561

562

563



564

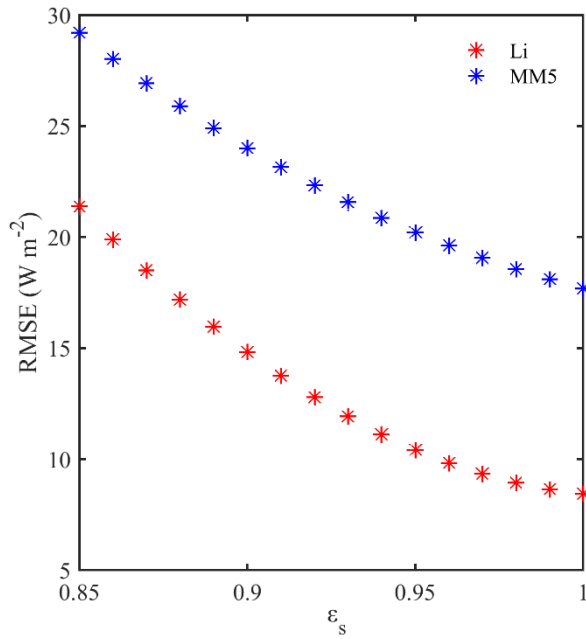
565 **Figure 2.** Wind Rose map at Gucheng station from December 1, 2016 to January 9, 2017.

566

567

568

569



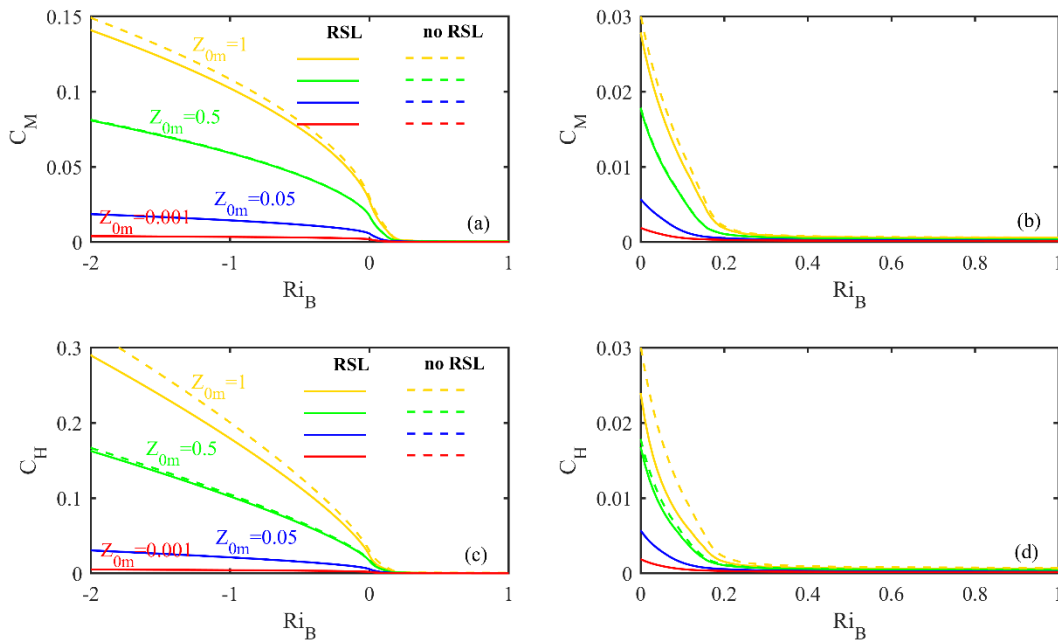
570

571 **Figure 3.** The surface emissivity ε_s dependence of RMSE between observed near-neutral heat fluxes and parameterized heat
 572 fluxes (red for Li and blue for MM5) at Gucheng station.

573

574

575

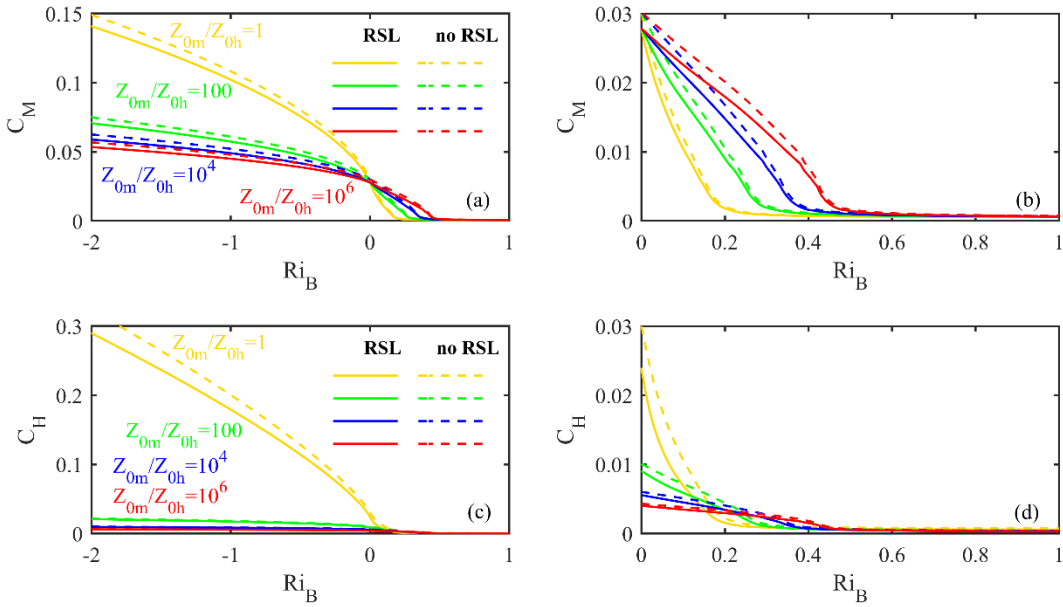


576

577

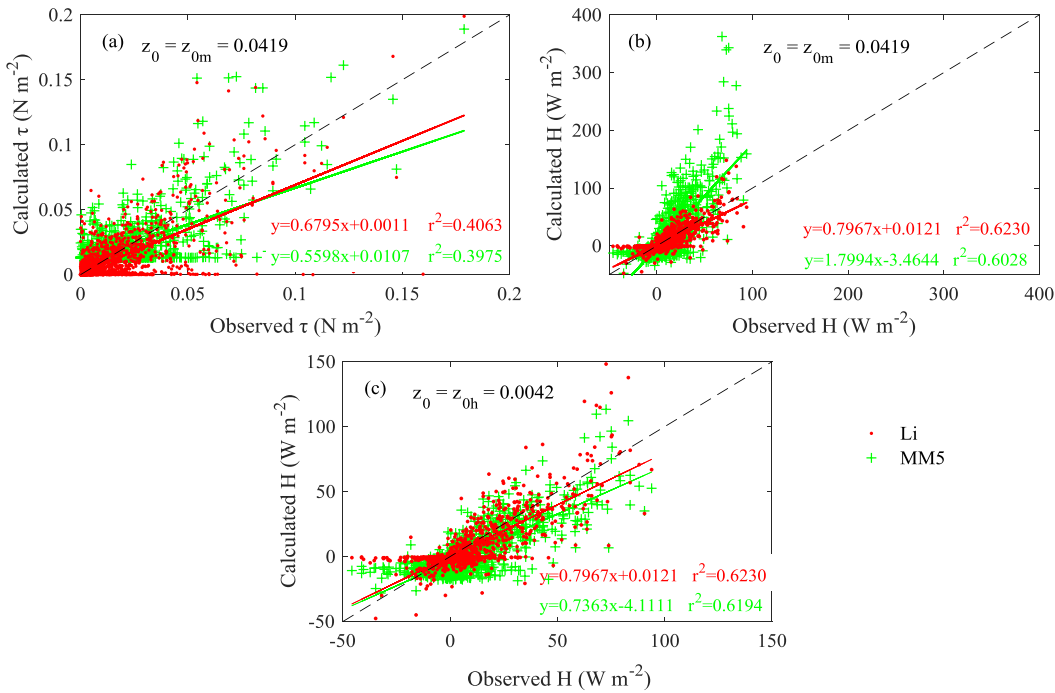
578 **Figure 4.** The relationships between $C_M(C_H)$ and Ri_B for under different z_{0m} values and treatments of RSL. Solid lines:
 579 considering the RSL effect; dotted lines: without the RSL effect.

579



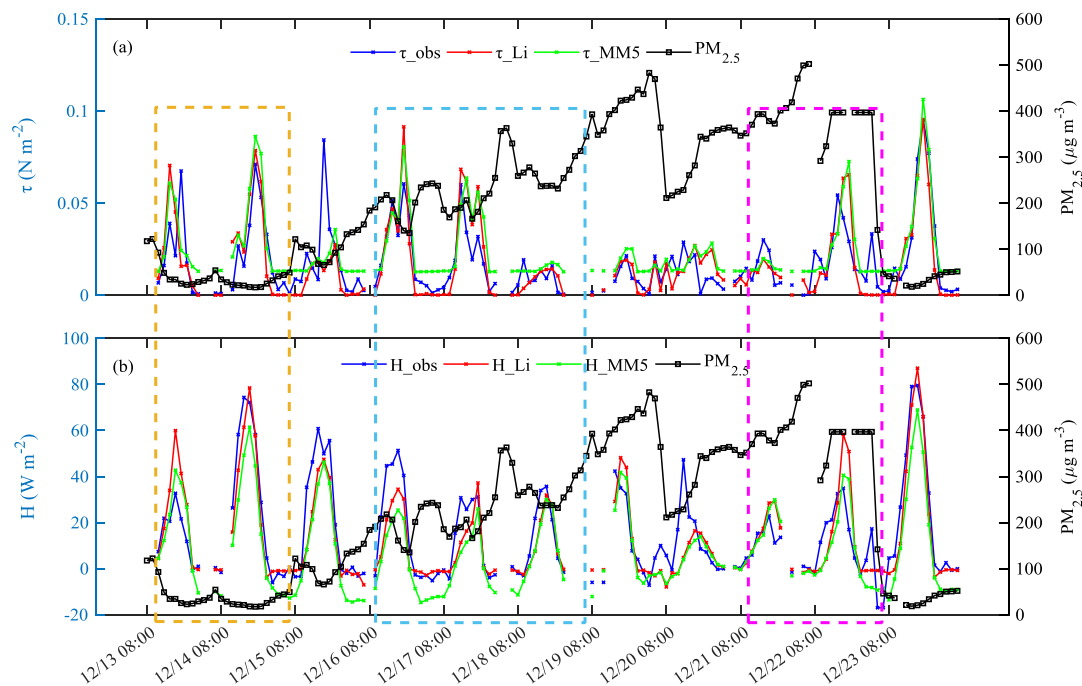
580
581
582
583
584
585
586

Figure 5. The relationships between C_M (C_H) and Ri_B for under different ratios of z_{0m} to z_{0h} and treatments of RSL. Solid lines: considering the RSL effect; dotted lines: without the RSL effect.



587
588
589
590
591
592

Figure 6. Comparison of calculated and observed fluxes at Gucheng station from December 1, 2016 to January 9, 2017. (a) Momentum fluxes (MM5: $z_0 = 0.0419$); (b) sensible heat fluxes (MM5: $z_0 = 0.0419$); (c) sensible heat fluxes (MM5: $z_0 = 0.0042$). Red dots: the Li scheme; green plus signs: the MM5 scheme.



595

596

Figure 7. Variations of hourly turbulent fluxes and observed $PM_{2.5}$ at Gucheng station in daytime. (a) Momentum fluxes τ

597

(blue line: observations; red line: the Li scheme; green line: the MM5 scheme) and $PM_{2.5}$ concentration (black line); (b) sensible

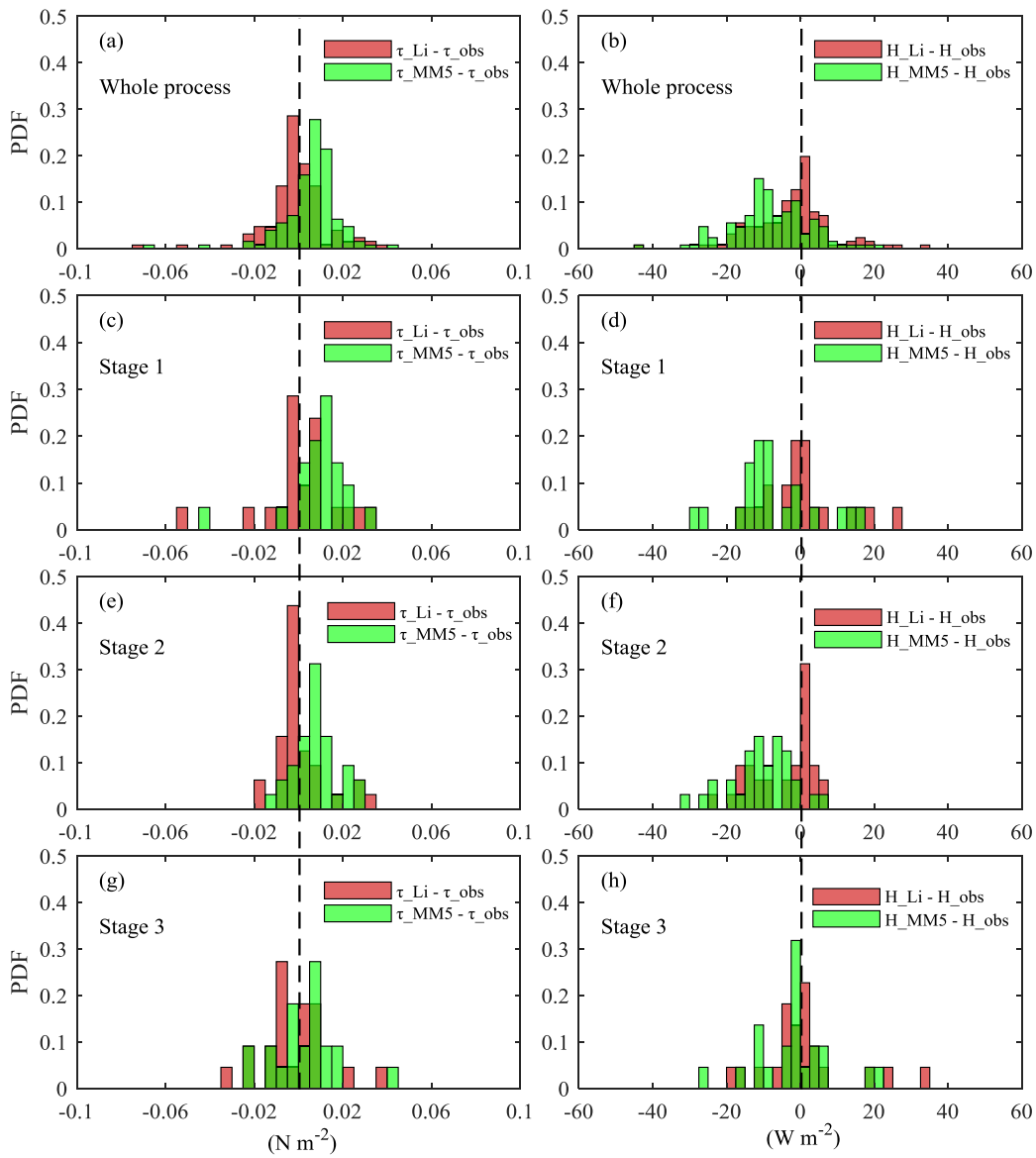
598

heat fluxes H (the same as τ) and $PM_{2.5}$ concentration (black line). Yellow box: stage 1; blue box: stage 2; purple box: stage 3.

599

600

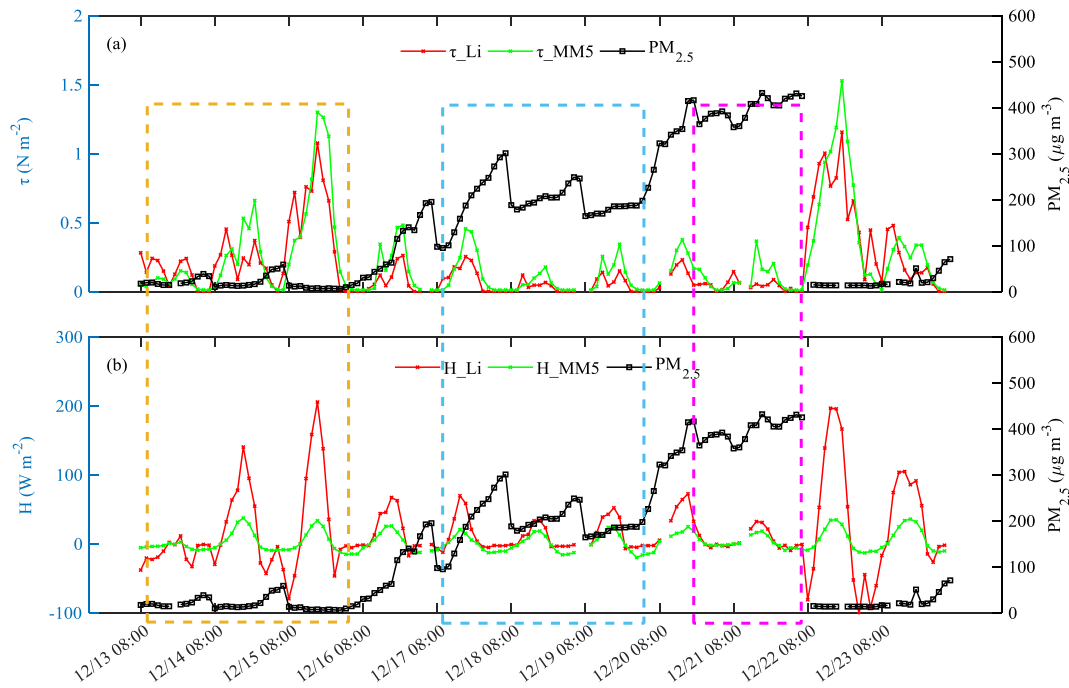
601



602

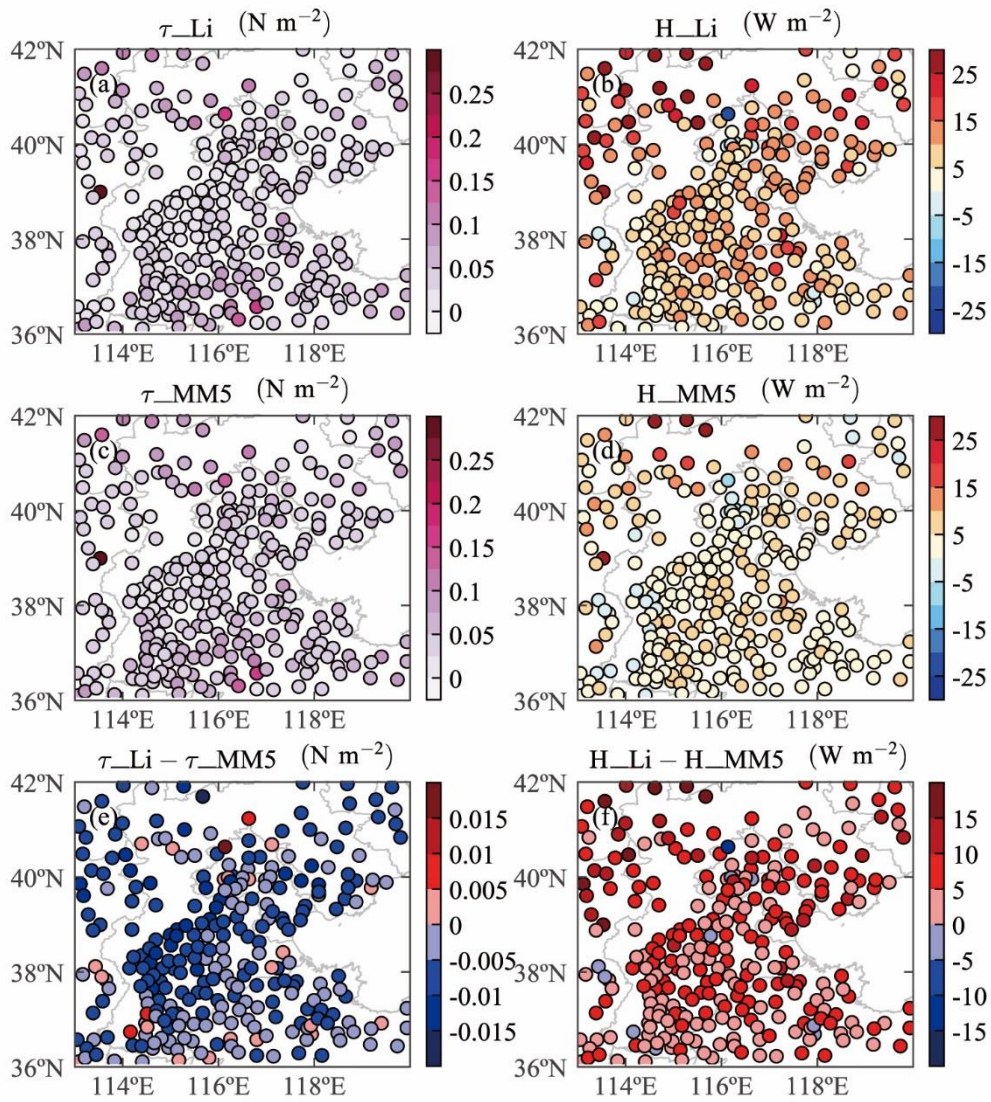
603 **Figure 8.** Probability distribution functions (PDF) of the differences between calculated fluxes (momentum fluxes: left;
 604 sensible heat fluxes: right) by using two schemes (the Li scheme: red bars; the MM5 scheme: green bars) and observations in
 605 different stages (a-b: whole process; c-d: stage 1; e-f: stage 2; g-h: stage 3).

606



607
 608 **Figure 9.** As in Fig. 7 but for Beijing station.

609
 610



611
 612 **Figure 10.** The mean momentum and sensible heat fluxes calculated by using two schemes (a-b: the Li scheme; c-d: the MM5
 613 scheme) and their differences (Li minus MM5; e: difference of the momentum fluxes; f: difference of the sensible heat fluxes)
 614 in Jing-Jin-Ji during the haze episode (December 13 to 23, 2016).